



MAX-PLANCK-INSTITUT
FÜR PLASMAPHYSIK

Projet de Recherche (PRe)

Spécialité : Mathématiques Appliquées

Année scolaire : 2024-2025

Contribution to the development of the Psydac
and Struphy finite element libraries.

Rapport Non-confidentiel et publiable sur Internet

Auteur : Arasu Candassamy

Promotion : 2026

Tuteur ENSTA :

SONIA FLISS

sonia.fliss@ensta.fr

Tuteur Organisme d'accueil :

MARTIN CAMPOS-PINTO

martin.campos-pinto@ipp.mpg.de

Stage effectué du 26/05/2025 au 22/08/2025

Nom de l'organisme d'accueil : Max-Planck-Institute Für Plasmaphysik

Adresse : Boltzmannstrasse 2, 85748 Garching bei München

Abstract

Lorem ipsum dolor sit amet, consectetuer adipiscing elit. Ut purus elit, vestibulum ut, placerat ac, adipiscing vitae, felis. Curabitur dictum gravida mauris. Nam arcu libero, nonummy eget, consectetuer id, vulputate a, magna. Donec vehicula augue eu neque. Pellentesque habitant morbi tristique senectus et netus et malesuada fames ac turpis egestas. Mauris ut leo. Cras viverra metus rhoncus sem. Nulla et lectus vestibulum urna fringilla ultrices. Phasellus eu tellus sit amet tortor gravida placerat. Integer sapien est, iaculis in, pretium quis, viverra ac, nunc. Praesent eget sem vel leo ultrices bibendum. Aenean faucibus. Morbi dolor nulla, malesuada eu, pulvinar at, mollis ac, nulla. Curabitur auctor semper nulla. Donec varius orci eget risus. Duis nibh mi, congue eu, accumsan eleifend, sagittis quis, diam. Duis eget orci sit amet orci dignissim rutrum.

Nam dui ligula, fringilla a, euismod sodales, sollicitudin vel, wisi. Morbi auctor lorem non justo. Nam lacus libero, pretium at, lobortis vitae, ultricies et, tellus. Donec aliquet, tortor sed accumsan bibendum, erat ligula aliquet magna, vitae ornare odio metus a mi. Morbi ac orci et nisl hendrerit mollis. Suspendisse ut massa. Cras nec ante. Pellentesque a nulla. Cum sociis natoque penatibus et magnis dis parturient montes, nascetur ridiculus mus. Aliquam tincidunt urna. Nulla ullamcorper vestibulum turpis. Pellentesque cursus luctus mauris.

Keywords:

Résumé

Lorem ipsum dolor sit amet, consectetuer adipiscing elit. Ut purus elit, vestibulum ut, placerat ac, adipiscing vitae, felis. Curabitur dictum gravida mauris. Nam arcu libero, nonummy eget, consectetuer id, vulputate a, magna. Donec vehicula augue eu neque. Pellentesque habitant morbi tristique senectus et netus et malesuada fames ac turpis egestas. Mauris ut leo. Cras viverra metus rhoncus sem. Nulla et lectus vestibulum urna fringilla ultrices. Phasellus eu tellus sit amet tortor gravida placerat. Integer sapien est, iaculis in, pretium quis, viverra ac, nunc. Praesent eget sem vel leo ultrices bibendum. Aenean faucibus. Morbi dolor nulla, malesuada eu, pulvinar at, mollis ac, nulla. Curabitur auctor semper nulla. Donec varius orci eget risus. Duis nibh mi, congue eu, accumsan eleifend, sagittis quis, diam. Duis eget orci sit amet orci dignissim rutrum.

Nam dui ligula, fringilla a, euismod sodales, sollicitudin vel, wisi. Morbi auctor lorem non justo. Nam lacus libero, pretium at, lobortis vitae, ultricies et, tellus. Donec aliquet, tortor sed accumsan bibendum, erat ligula aliquet magna, vitae ornare odio metus a mi. Morbi ac orci et nisl hendrerit mollis. Suspendisse ut massa. Cras nec ante. Pellentesque a nulla. Cum sociis natoque penatibus et magnis dis parturient montes, nascetur ridiculus mus. Aliquam tincidunt urna. Nulla ullamcorper vestibulum turpis. Pellentesque cursus luctus mauris.

Mots-clés:

Acknowledgement

 Lorem ipsum dolor sit amet, consectetuer adipiscing elit. Ut purus elit, vestibulum ut, placerat ac, adipiscing vitae, felis. Curabitur dictum gravida mauris. Nam arcu libero, nonummy eget, consectetuer id, vulputate a, magna. Donec vehicula augue eu neque. Pellentesque habitant morbi tristique senectus et netus et malesuada fames ac turpis egestas. Mauris ut leo. Cras viverra metus rhoncus sem. Nulla et lectus vestibulum urna fringilla ultrices. Phasellus eu tellus sit amet tortor gravida placerat. Integer sapien est, iaculis in, pretium quis, viverra ac, nunc. Praesent eget sem vel leo ultrices bibendum. Aenean faucibus. Morbi dolor nulla, malesuada eu, pulvinar at, mollis ac, nulla. Curabitur auctor semper nulla. Donec varius orci eget risus. Duis nibh mi, congue eu, accumsan eleifend, sagittis quis, diam. Duis eget orci sit amet orci dignissim rutrum.

 Nam dui ligula, fringilla a, euismod sodales, sollicitudin vel, wisi. Morbi auctor lorem non justo. Nam lacus libero, pretium at, lobortis vitae, ultricies et, tellus. Donec aliquet, tortor sed accumsan bibendum, erat ligula aliquet magna, vitae ornare odio metus a mi. Morbi ac orci et nisl hendrerit mollis. Suspendisse ut massa. Cras nec ante. Pellentesque a nulla. Cum sociis natoque penatibus et magnis dis parturient montes, nascetur ridiculus mus. Aliquam tincidunt urna. Nulla ullamcorper vestibulum turpis. Pellentesque cursus luctus mauris.

Contents

Abstract	3
Acknowledgement	5
1 Introduction	7
2 Linear Elasticity	8
2.1 Physical Model and Strong Formulation	8
2.2 Pure displacement weak-formulation	9
2.3 Numerical simulation using PSYDAC on the Supercomputer Raven	11
2.3.1 Dirichlet Homogeneous Boundary conditions on $\partial\Omega_D = \partial\Omega$	12
2.3.2 Mixed boundary conditions	15
2.4 Mixed displacement-pressure formulation	18
2.4.1 Example of simulation using PSYDAC	18
3 References	21
4 Appendices	22
4.1 Other plots of solutions for the problem with Dirichlet Homogeneous Boundary Conditions	22

Chapter 1

Introduction

The Max-Planck Institute for Plasma Physics (IPP), located in Garching and Greifswald, is a renowned research institute in Plasma physics and Nuclear fusion. Founded under the Max-Planck Society in 1960, this institute has a long tradition of scientific excellence and innovation. The Department of Numerical Methods for Plasma Physics (NMPP), where my internship took place, plays a crucial role in developing advanced simulation techniques to understand and predict the behavior of plasmas in complex environments (in tokamaks or stelarators).

The Finite Element Method (FEM) is a widely used numerical technique for solving Partial Differential Equations (PDEs). It is particularly well-suited for addressing plasma physics problems due to its ability to handle complex geometries and varied boundary conditions. FEM allows for the discretization of a continuous domain into a set of finite elements, thereby facilitating the numerical resolution of equations governing the physical phenomena under study.

In the context of electromagnetism, the Finite Element Exterior Calculus (FEEC) formulation is a powerful approach for solving Maxwell's equations. This method is particularly suitable for problems involving electromagnetic fields, as it preserves certain topological and physical properties of the original equations. FEEC provides a powerfull framework for plasma simulation, where electromagnetic interactions play a central role.

Psydac is an integrated development environment (IDE) specifically designed for simulation and data analysis in plasma physics. It offers a range of tools to facilitate the implementation of numerical methods, including FEM and FEEC frameworks. Psydac enables researchers to develop complex models, simulate them, and analyze results efficiently and intuitively. Psydac also stands out as an isogeometric analysis library, an approach that integrates geometric modeling and numerical analysis within a unified framework. Isogeometric analysis allows simulations to be performed directly on the geometric models used for design, eliminating the need to convert CAD models into traditional meshes for simulations. This provides increased accuracy and better integration between design and analysis, reducing errors and improving the efficiency of the simulation process. Using Psydac, researchers can leverage these capabilities to develop more accurate models and perform more reliable analyses, which is particularly advantageous in the complex field of plasma physics.

This internship report describes my experience and contributions within the NMPP Department at the IPP. Psydac should be able to solve any PDEs but it hasn't been tested on equations from solid mechanics. Then, during this internship, I have explored the linear elasticity problem, its simulation using Psydac and its running on Supercomputer Raven.

Chapter 2

Linear Elasticity

2.1 Physical Model and Strong Formulation

The following presentation of the context of work and physical background comes from [Gou13] and [EG04].

Let's denote by $\Omega \subset \mathbb{R}^3$ a deformable medium characterized by λ and μ Lamé's coefficient ($\lambda, \mu > 0$). Ω is a bounded open domain with lipschitzian boundary. λ is called Lamé's first coefficient, μ is the shear modulus. These coefficient are related to the Young modulus and Poisson coefficient of the medium. The deformable medium is under an external load $\vec{f} : \Omega \rightarrow \mathbb{R}^3$. Then, we are looking for $\vec{u} : \Omega \rightarrow \mathbb{R}^3$ the displacement field, when the equilibrium is reached.

The material verifies the following equilibrium condition :

$$\nabla \cdot \boldsymbol{\sigma}(\vec{u}) + \vec{f} = \vec{0} \text{ in } \Omega, \quad (2.1)$$

where $\boldsymbol{\sigma}(\vec{u})$ is the Cauchy Stress Tensor, defined by $\boldsymbol{\sigma}(\vec{u}) = C : \boldsymbol{\varepsilon}(\vec{u})$. C is the fourth-order stiffness tensor and

$$\boldsymbol{\varepsilon}(\vec{u}) := \frac{1}{2}(\nabla \vec{u} + (\nabla \vec{u})^T)$$

is the strain tensor. In the context of linear elasticity, the relation between $\boldsymbol{\varepsilon}(\vec{u})$ and $\boldsymbol{\sigma}(\vec{u})$ is simpler :

$$\boldsymbol{\sigma}(\vec{u}) = \lambda \operatorname{Tr}(\boldsymbol{\varepsilon}) I_3 + 2\mu \boldsymbol{\varepsilon} = \lambda(\nabla \cdot \vec{u}) I_3 + \mu(\nabla \vec{u} + (\nabla \vec{u})^T) \text{ in } \Omega. \quad (2.2)$$

For boundary conditions, there are two types of boundary conditions : Dirichlet conditions on the displacement field \vec{u} and Traction conditions on the Cauchy Stress Tensor $\boldsymbol{\sigma}(\vec{u})$.

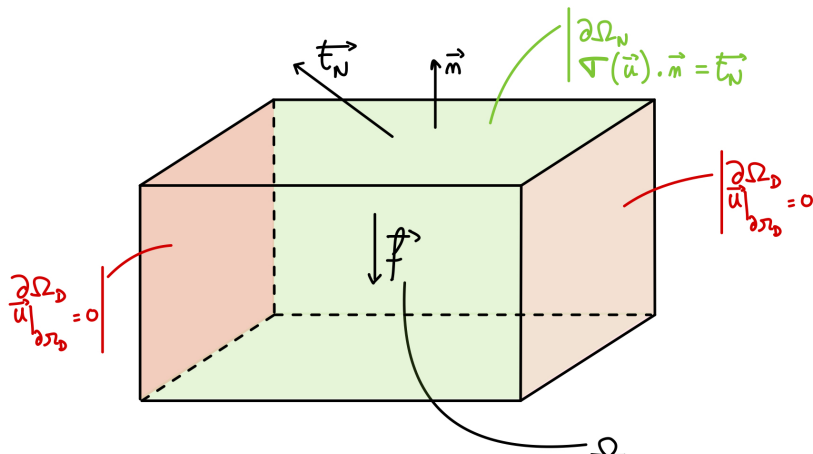


Figure 2.1: Representation of a domain Ω

Let's decompose $\partial\Omega$ as $\partial\Omega_D$ and $\partial\Omega_N$ such that $\partial\Omega_D \cup \partial\Omega_N = \partial\Omega$, $\partial\Omega_D \cap \partial\Omega_N = \emptyset$. Let's denote by $\vec{t}_N : \partial\Omega_N \rightarrow \mathbb{R}^3$ the normal traction force and \vec{n} the normal vector of $\partial\Omega$ outside-oriented. We can consider the boundary displacement on $\partial\Omega_D$ as equal to $\vec{0}$.

In case of non-homogenous boundary conditions $\vec{g} : \partial\Omega_D \rightarrow \mathbb{R}^3$, we can solve the problem for $\vec{u} - \vec{g}$ by modifying the source term. Then, the solution of linear elasticity problem should verify :

$$\begin{cases} \vec{u} = \vec{0} & \partial\Omega_D \\ \boldsymbol{\sigma}(\vec{u}) \cdot \vec{n} = \vec{t}_N & \partial\Omega_N \end{cases}$$

Physically, \vec{f} is a "volume force" on Ω and \vec{t}_N is a "surface force". The strong formulation of this problem is :

For a given $\vec{f} \in \mathbf{L}^2(\Omega)$, $\vec{t}_N \in \mathbf{L}^2(\partial\Omega_N)$, find $\vec{u} \in \mathbf{H}^1(\Omega)$ such that :

$$\begin{cases} -\nabla \cdot \boldsymbol{\sigma}(\vec{u}) = \vec{f} & \text{in } \Omega \quad (\text{Equilibrium}) \\ \boldsymbol{\sigma}(\vec{u}) = \lambda(\nabla \cdot \vec{u})I_3 + \mu(\nabla \vec{u} + (\nabla \vec{u})^T) & \text{in } \Omega \quad (\text{Hook's law}) \\ \vec{u} = \vec{0} & \text{in } \partial\Omega_D \\ \boldsymbol{\sigma}(\vec{u}) \cdot \vec{n} = \vec{t}_N & \text{in } \partial\Omega_N \end{cases} \quad (2.3)$$

where $\mathbf{L}^2(\Omega) = (L^2(\Omega))^3$, $\mathbf{L}^2(\partial\Omega_N) = (L^2(\partial\Omega_N))^3$, $\mathbf{H}^1(\Omega) = (H^1(\Omega))^3$,

2.2 Pure displacement weak-formulation

To derive the weak formulation from (2.3), let's introduce the following functionnal space :

$$\mathbf{H}_{\vec{0},D}^1(\Omega) = \left\{ \vec{v} \in \mathbf{H}^1(\Omega) \mid \vec{v}|_{\partial\Omega_D} = \vec{0} \right\},$$

which is a sub-hilbert space of $\mathbf{H}^1(\Omega)$ equipped with the same dot product (as a closed space of a Hilbert space). By taking the scalar product of the equilibrium equation from (2.3) with $\vec{v} \in (H_{\vec{0},D}^1(\Omega))^3$ and applying a Green's formula, one gets that :

$$\int_{\Omega} \boldsymbol{\sigma}(\vec{u}) : (\nabla \vec{v}) dV - \int_{\partial\Omega} (\boldsymbol{\sigma}(\vec{u}) \cdot \vec{n}) \cdot \vec{v} dS = \int_{\Omega} \vec{f} \cdot \vec{v} dV$$

One can remark that with (2.2), the tensor $\boldsymbol{\sigma}(\vec{u})$ is symetric. It implies that :

$$\boldsymbol{\sigma}(\vec{u}) : \nabla \vec{v} = \boldsymbol{\sigma}(\vec{u}) : \boldsymbol{\epsilon}(\vec{v})$$

Moreover, $\vec{v} \in (H_{\vec{0},D}^1(\Omega))^3$, then $\vec{v}|_{\partial\Omega_D} = \vec{0}$. So the weak formulation can be simplified into :

$$\begin{cases} \text{Find } \vec{u} \in \mathbf{H}_{\vec{0},D}^1(\Omega) \text{ such that :} \\ a(\vec{u}, \vec{v}) = l(\vec{v}) \quad \forall \vec{v} \in \mathbf{H}_{\vec{0},D}^1(\Omega) \end{cases} \quad (2.4)$$

With :

$$\begin{aligned} a : & \left\{ \begin{array}{l} \mathbf{H}_{\vec{0},D}^1(\Omega) \times \mathbf{H}_{\vec{0},D}^1(\Omega) \rightarrow \mathbb{R} \\ (\vec{u}, \vec{v}) \mapsto \int_{\Omega} \boldsymbol{\sigma}(\vec{u}) : \boldsymbol{\epsilon}(\vec{v}) dV = \int_{\Omega} \lambda(\nabla \cdot \vec{u})(\nabla \cdot \vec{v}) dV + \int_{\Omega} 2\mu \boldsymbol{\epsilon}(\vec{u}) : \boldsymbol{\epsilon}(\vec{v}) dV \end{array} \right. \\ l : & \left\{ \begin{array}{l} \mathbf{H}_{\vec{0},D}^1(\Omega) \rightarrow \mathbb{R} \\ \vec{v} \mapsto \int_{\Omega} \vec{f} \cdot \vec{v} dV + \int_{\partial\Omega_N} \vec{t}_N \cdot \vec{v} dS \end{array} \right. \end{aligned}$$

In continuum mechanics, (2.4) is called the Principle of Virtual Work. Let's look at the well-posedness of (2.4). Before starting, let's remind some notations and lemmas.

$\|\cdot\|_{\mathbf{H}^1(\Omega)}$ is defined as : $\forall \vec{v} \in \mathbf{H}^1(\Omega), \|\vec{v}\|_{\mathbf{H}^1(\Omega)} = \left(\sum_{i=1}^3 \|v_i\|_{H^1(\Omega)} \right)^{1/2}$.

Lemma 2.2.1. 1. $\forall \vec{u} \in \mathbf{H}^1(\Omega)$,

$$\int_{\Omega} (\nabla \cdot \vec{u})^2 dV \leq 3 \|\vec{u}\|_{\mathbf{H}^1(\Omega)}^2$$

2. $\forall \vec{u} \in \mathbf{H}^1(\Omega)$,

$$\boldsymbol{\varepsilon}(\vec{u}) : \boldsymbol{\varepsilon}(\vec{u}) \leq \nabla \vec{u} : \nabla \vec{u}$$

Then :

$$\int_{\Omega} \boldsymbol{\varepsilon}(\vec{u}) : \boldsymbol{\varepsilon}(\vec{u}) d\Omega \leq \int_{\Omega} \nabla \vec{u} : \nabla \vec{u} d\Omega \leq \|\vec{u}\|_{\mathbf{H}^1(\Omega)}^2$$

Proof. By calculus, or a detailed version in [Cin18] □

Lemma 2.2.2. (*First Korn's inequality*)

Let $\Omega \subset \mathbb{R}^3$ a domain and denotes by $\|\boldsymbol{\varepsilon}(\vec{u})\|_{\mathbf{L}^2(\Omega)} := (\int_{\Omega} \boldsymbol{\varepsilon}(\vec{u}) : \boldsymbol{\varepsilon}(\vec{u}))^{1/2}$. Then, there exists $C > 0$ such that:

$$\forall \vec{v} \in \mathbf{H}_{\vec{0}}^1(\Omega), \quad C \|\vec{v}\|_{\mathbf{H}^1(\Omega)} \leq \|\boldsymbol{\varepsilon}(\vec{v})\|_{\mathbf{L}^2(\Omega)}$$

Proof. A proof can be found in [BS08] □

Lemma 2.2.3. (*Second Korn's inequality*)

Let $\Omega \subset \mathbb{R}^3$ a domain. Then, there exists $C > 0$ such that:

$$\forall \vec{v} \in \mathbf{H}^1(\Omega), \quad C \|\vec{v}\|_{\mathbf{H}^1(\Omega)} \leq \|\boldsymbol{\varepsilon}(\vec{v})\|_{\mathbf{L}^2(\Omega)} + \|\vec{v}\|_{\mathbf{L}^2(\Omega)}$$

By Rellich theorem, $\mathbf{H}^1(\Omega)$ is compactly embedded in $\mathbf{L}^2(\Omega)$ as Ω is a open bounded domain . Then, one can show that there exists $C > 0$ such that:

$$\forall \vec{v} \in \mathbf{H}^1(\Omega), \quad C \|\vec{v}\|_{\mathbf{H}^1(\Omega)} \leq \|\boldsymbol{\varepsilon}(\vec{v})\|_{\mathbf{L}^2(\Omega)}$$

Proof. A proof can be found in [BS08] □

Now, we can prove the well-posedness of (2.4) when $|\Omega_D| > 0$.

- $(\mathbf{H}_{\vec{0},D}^1(\Omega), \|\cdot\|_{\mathbf{H}^1(\Omega)})$ is a Hilbert space.
- $a(\cdot, \cdot)$ is a bilinear form on $\mathbf{H}_{\vec{0},D}^1(\Omega) \times \mathbf{H}_{\vec{0},D}^1(\Omega)$ and $l(\cdot)$ a linear form on $\mathbf{H}_{\vec{0},D}^1(\Omega)$.
- $l(\cdot)$ is continuous :

$$\begin{aligned} \forall \vec{v} \in \mathbf{H}_{\vec{0},D}^1(\Omega), |l(\vec{v})| &\leq \left| (\vec{f}, \vec{v})_{\mathbf{L}^2(\Omega)} + (\vec{t}_N, \vec{v})_{\mathbf{L}^2(\partial\Omega_N)} \right| \\ |l(\vec{v})| &\leq \left(\|\vec{f}\|_{\mathbf{L}^2(\Omega)} + \|\gamma_0\| \|\vec{t}_N\|_{\mathbf{L}^2(\partial\Omega_N)} \right) \|\vec{v}\|_{\mathbf{H}^1(\Omega)} \end{aligned}$$

- $a(\cdot, \cdot)$ is continuous:

$$\forall \vec{u}, \vec{v} \in \mathbf{H}_{\vec{0},D}^1(\Omega), |a(\vec{u}, \vec{v})| \leq |a(\vec{u}, \vec{u})|^{1/2} |a(\vec{v}, \vec{v})|^{1/2}$$

By Cauchy-Schwarz Inequality as $a(\cdot, \cdot)$ is a symmetric and positive bilinear form

$$|a(\vec{u}, \vec{v})| \leq (3\lambda + 2\mu) \|\vec{u}\|_{\mathbf{H}^1(\Omega)} \|\vec{v}\|_{\mathbf{H}^1(\Omega)}.$$

- $a(.,.)$ is coercive:

– If $\Omega_D = \Omega$, then $\mathbf{H}_{0,D}^1(\Omega) = \mathbf{H}_0^1(\Omega)$ and we can apply **Lemma 2.2.2** : there exists $C > 0$ such that:

$$\begin{aligned}\forall \vec{u} \in \mathbf{H}_{0,D}^1(\Omega), \quad a(u, u) &= \int_{\Omega} \lambda (\nabla \cdot \vec{u})^2 dV + \int_{\Omega} 2\mu \boldsymbol{\varepsilon}(\vec{u}) : \boldsymbol{\varepsilon}(\vec{u}) dV \\ &\geq 2\mu \|\boldsymbol{\varepsilon}(\vec{u})\|_{L^2(\Omega)} \\ a(u, u) &\geq 2\mu C \|\vec{u}\|_{\mathbf{H}^1(\Omega)}\end{aligned}$$

– If $\Omega_D \subsetneq \Omega$, we can now apply **Lemma 2.2.3** : there exists $C > 0$ such that:

$$\forall \vec{u} \in \mathbf{H}_{0,D}^1(\Omega), \quad a(u, u) \geq 2\mu C \|\vec{u}\|_{\mathbf{H}^1(\Omega)}$$

Then, by Lax-Milgram theorem, the problem (2.4) is well-posed when $|\Omega_D| > 0$. When, $|\Omega_D| = 0$, (2.4) turns into the **Pure Traction Problem** :

$$\left\{ \begin{array}{l} \text{Find } \vec{u} \in \mathbf{H}^1(\Omega) \text{ such that :} \\ a(\vec{u}, \vec{v}) = \int_{\Omega} \vec{f} \cdot \vec{v} dV + \int_{\partial\Omega} \vec{t}_N \cdot \vec{v} dS =: l(\vec{v}) \quad \forall \vec{v} \in \mathbf{H}^1(\Omega) \end{array} \right. \quad (2.5)$$

This problem isn't really well-posed. Regarding to the Rigid Displacement Field (translations and rotations) $\mathcal{R} = \left\{ \vec{v} \in \mathbf{H}^1(\Omega) \mid \exists x_1, x_2 \in \mathbb{R}^3, \vec{v}(x) = x_1 + x_2 \times x \right\}$,

$$\forall \vec{v} \in \mathcal{R}, \quad \nabla \cdot \vec{v} = 0 \text{ and } \boldsymbol{\varepsilon}(\vec{v}) = 0.$$

Then :

$$\forall \vec{u} \in \mathbf{H}^1(\Omega), \forall \vec{v} \in \mathcal{R}, \quad a(\vec{u}, \vec{v}) = 0.$$

So, the weak formulation (2.5) is solvable iff the following compatibility equality holds :

$$\forall \vec{v} \in \mathcal{R}, \quad \int_{\Omega} \vec{f} \cdot \vec{v} dV + \int_{\partial\Omega} \vec{t}_N \cdot \vec{v} dS = 0,$$

and in this case, there exists an unique solution $\vec{u} \in \hat{\mathbf{H}}^1(\Omega) := \left\{ \vec{v} \in \mathbf{H}^1(\Omega) \mid \int_{\Omega} \vec{v} dV = \int_{\Omega} \nabla \times \vec{v} dV = \vec{0} \right\}$
 In case of **Pure Traction Problem**, we are looking for a solution modulo a rigid displacement field.
A more rigorous proof of the equivalence can be found in [BS08] and [Che24].

2.3 Numerical simulation using PSYDAC on the Supercomputer Raven

PSYDAC is high-level programming IDE and very intuitive to use. It is using SymPDE and Pyccel. SymPDE implements in Python abstract objects (Functionnal Space, differential operators, linear and bilinear forms...). Pyccel is a transpiler, used to convert a Python Code into a C or Fortran code, in order to take advantage from code acceleration and parallelization. The figure 2.2 summarize the dependancy between PSYDAC, SymPDE and Pyccel. A more detailed presentation of PSYDAC can be found in [GHR22].

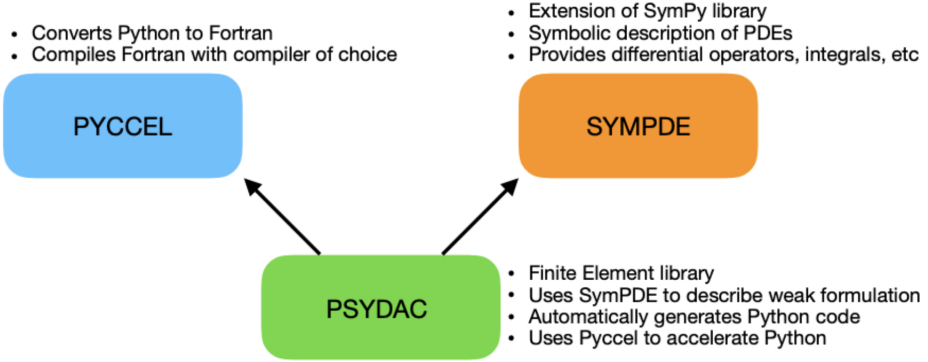


Figure 2.2: Dependancy graph of PSYDAC, from [GHR22]

Raven is a supercomputer located at the Max-Planck Institute for Plasma Physics. It is part of the High Performance Computing (HPC) infrastructure and is used for large-scale simulations and data analysis in plasma physics and related fields. I had the opportunity to run my simulations on Raven, which provided me with access to powerful computational resources and parallel processing capabilities.

2.3.1 Dirichlet Homogeneous Boundary conditions on $\partial\Omega_D = \partial\Omega$

In a first time, to get the grips with PSYDAC and the HPC, I have considered the case $\Omega = [0, 1]^3$, $\partial\Omega_D = \partial\Omega$ and $\partial\Omega_N = \emptyset$. To verify if the numerical resolution of PSYDAC of (2.4) is correct, I have used the Method of Manufactured Solutions. The concept is quite simpler, we assume that a function $\vec{u}_e \in \mathbf{H}_0^1(\Omega)$ verifies the strong problem (2.3), then we compute the source term \vec{f} and we solve the (2.4) with \vec{f} as a source term and we look at the error between the numerical solution and the theoretical one. I have considered \vec{u}_e defined as :

$$\vec{u}_e = \begin{pmatrix} 0 \\ 0 \\ \sin(\pi x) \sin(\pi y) \sin(\pi z) \end{pmatrix} \in \mathbf{H}_0^1(\Omega).$$

Then, we can compute manually the source term \vec{f} :

$$\vec{f} = \begin{pmatrix} -\pi^2 (\lambda + \mu) \sin(y) \cos(\pi x) \cos(\pi z) \\ -\pi^2 (\lambda + \mu) \sin(\pi x) \cos(y) \cos(\pi z) \\ \pi^2 (\lambda + 4\mu) \sin(\pi x) \sin(\pi y) \sin(\pi z) \end{pmatrix} \in \mathbf{L}^2(\Omega).$$

To make the numerical simulation with PSYDAC, we have to choose two important parameters : d the maximum degree of B-Splines functions that will approximate the solution and n_{cells} is the number of cells in each dimension of Ω for the finite dimensional space. $h \propto \frac{1}{n_{\text{cells}}}$, an usual discretization parameters for finite dimensional spaces and d will conduct the convergence speed of the numerical solution. By solving the problem Dirichlet Homogeneous Boundary conditions on the whole border, one can observe the following plots of the simulated $\vec{u}_{e,3}^h$ for different plane z . It is possible to plot also the error $\vec{u}_{e,3} - \vec{u}_{e,3}^h$.

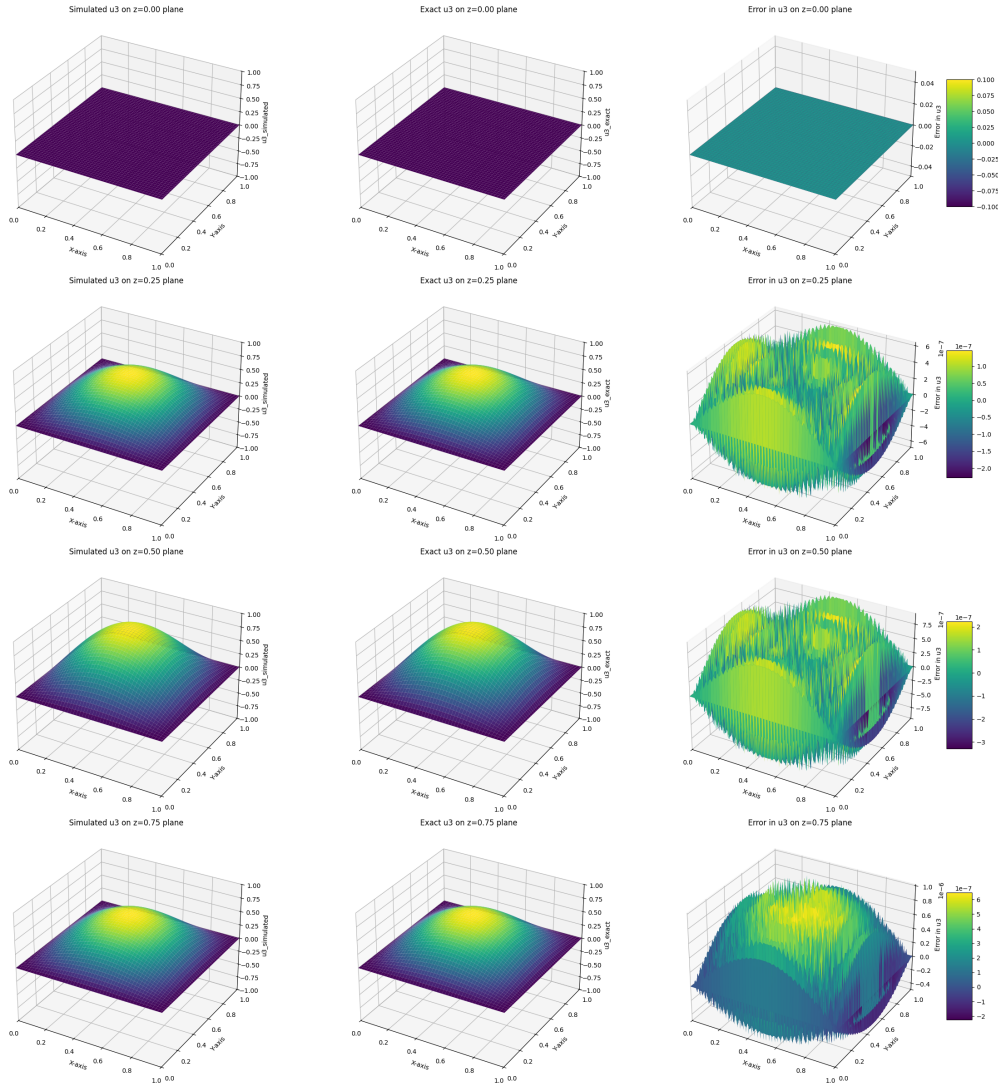


Figure 2.3: Plots comparison between the simulated and real $u_{e,3}$ with the error, for different plane z , with $d = 2$ and $n_{\text{cell}} = 64$

We can observe that the numerical solution is "quite" near the real solution. To get a better estimation of convergence rate, let's look at the Céa's lemma in this case.

Denotes by $\mathbf{V}^h \subset \mathbf{H}^1(\Omega)$ the discrete finite dimensional space, $\vec{u} \in \mathbf{H}^{s+1}(\Omega) \subset \mathbf{H}^1(\Omega)$, $1 \leq s \leq d + 1$ the real solution solution and $\vec{u}^h \in \mathbf{V}^h$ the discrete solution. Then, the Céa's lemma gives the following estimates :

$$\|\vec{u} - \vec{u}^h\|_{\mathbf{H}^1(\Omega)} \leq \frac{3\lambda + 2\mu}{2\mu C} \inf_{\vec{v}^h \in \mathbf{H}^1(\Omega)} \|\vec{u} - \vec{v}^h\|_{\mathbf{H}^1(\Omega)}$$

where $C > 0$ is a constant from Korn's inequality (independant of h). By applying **Corollary 4.21**, **4.27**, **Theorem 6.2** from [Da +14] and Aubin-Nitsche theorem, we can get the following estimates :

$$\begin{aligned} \|\vec{u} - \vec{u}^h\|_{\mathbf{H}^1(\Omega)} &\lesssim \frac{3\lambda + 2\mu}{2\mu C} h^q \|\vec{u}\|_{\mathbf{H}^{q+1}(\Omega)} \\ \|\vec{u} - \vec{u}^h\|_{L^2(\Omega)} &\lesssim (3\lambda + 2\mu) h^{q+1} \|\vec{u}\|_{\mathbf{H}^{q+1}(\Omega)} \end{aligned} \tag{2.6}$$

where $q = \min(s, d)$. In this case, u_e is an infinitely smooth solution, then $q = d$.

We can see that the numerical solution converges with the expected order to the real solution : the more the mesh is refined, the more the error is lower and the more the splines' degree is higher, the more the convergence rate is higher. For this numerical resolution, I have used **GMRES** method

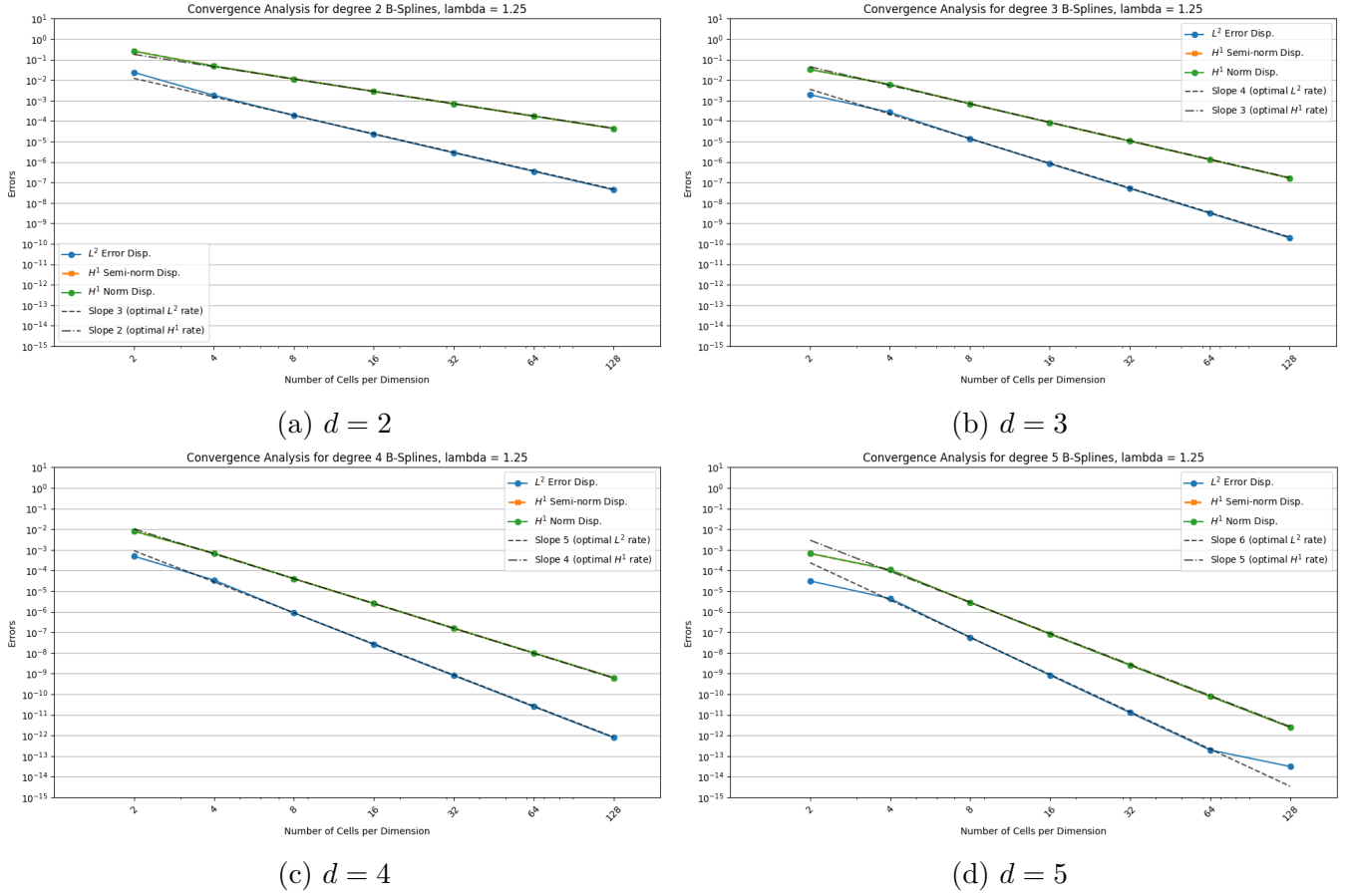


Figure 2.4: Four plots of relative errors ($\|\vec{u} - \vec{u}^h\|_{H^1(\Omega)}$ and $\|\vec{u} - \vec{u}^h\|_{L^2(\Omega)}$) with different degree B-Splines (with $\lambda = 1.25$ & $\mu = 1$)

to solve the linear system at the end of the discretization. That needed to take care of the tolerance of the solver, because with a fixed tolerance, if the d and n_{cells} are "too higher", the convergence rate cannot hold. The following figure illustrates this case, when $d = 5$ and $n_{\text{cells}} = 16$.

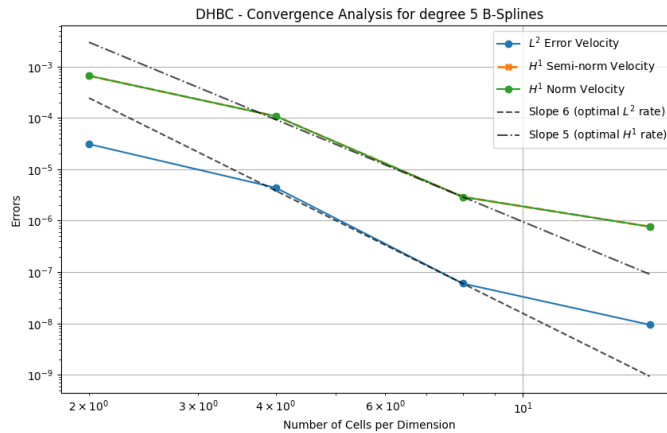


Figure 2.5: Error plot between exact and numerical solution with degree 5 B-Splines with "higher" tolerance for the solvera

But even with a lower tolerance for the solver (10^{-15} for figure 2.4d), the error reaches a plateau, which is not the case for lower degree B-Splines (at least for the tested configurations). This plateau can be explained by the matrix of the bilinear form $a(.,.)$ which is ill-conditioned. Moreover, the bad conditioning can become worse with more refined mesh and higher degree B-Splines (as the

convergence is faster).

2.3.2 Mixed boundary conditions

Then, I have made a simulation with Mixed Boundary Conditions, as it is introduced in (2.3), with also non-homogeneous Dirichlet boundary conditions.

Again, $\Omega = [0, 1]^3$, with :

$$\begin{aligned}\partial\Omega_{\text{DH}} &= \{(x, y, z) \in \partial\Omega \mid z = 0 \text{ or } z = 1\} & \partial\Omega_{\text{DNH}} &= \{(x, y, z) \in \partial\Omega \mid x = 0 \text{ or } x = 1\} \\ \partial\Omega_{\text{N}} &= \{(x, y, z) \in \partial\Omega \mid y = 0 \text{ or } y = 1\}\end{aligned}$$

For that purpose, \vec{u}_e , \vec{f} , \vec{t}_N and \vec{g} are now defined as :

$$\begin{aligned}\vec{u}_e &= \begin{pmatrix} 0 \\ 0 \\ \sin(\pi z) \cos(\pi x) \cos(\pi y) \end{pmatrix}, \vec{f} = \begin{pmatrix} \pi^2 (\lambda + \mu) \sin(\pi x) \cos(\pi y) \cos(\pi z) \\ \pi^2 (\lambda + \mu) \sin(\pi y) \cos(\pi x) \cos(\pi z) \\ \pi^2 (\lambda + 4\mu) \sin(\pi z) \cos(\pi x) \cos(\pi y) \end{pmatrix} \\ \vec{t}_N &= \begin{pmatrix} 0 \\ -\lambda \pi \cos(\pi x) \cos(\pi z) \\ 0 \end{pmatrix}, \vec{g} = \begin{pmatrix} 0 \\ 0 \\ \pm \sin(\pi z) \cos(\pi y) \end{pmatrix}\end{aligned}$$

Then, we can get the same plots and interpretation as before.

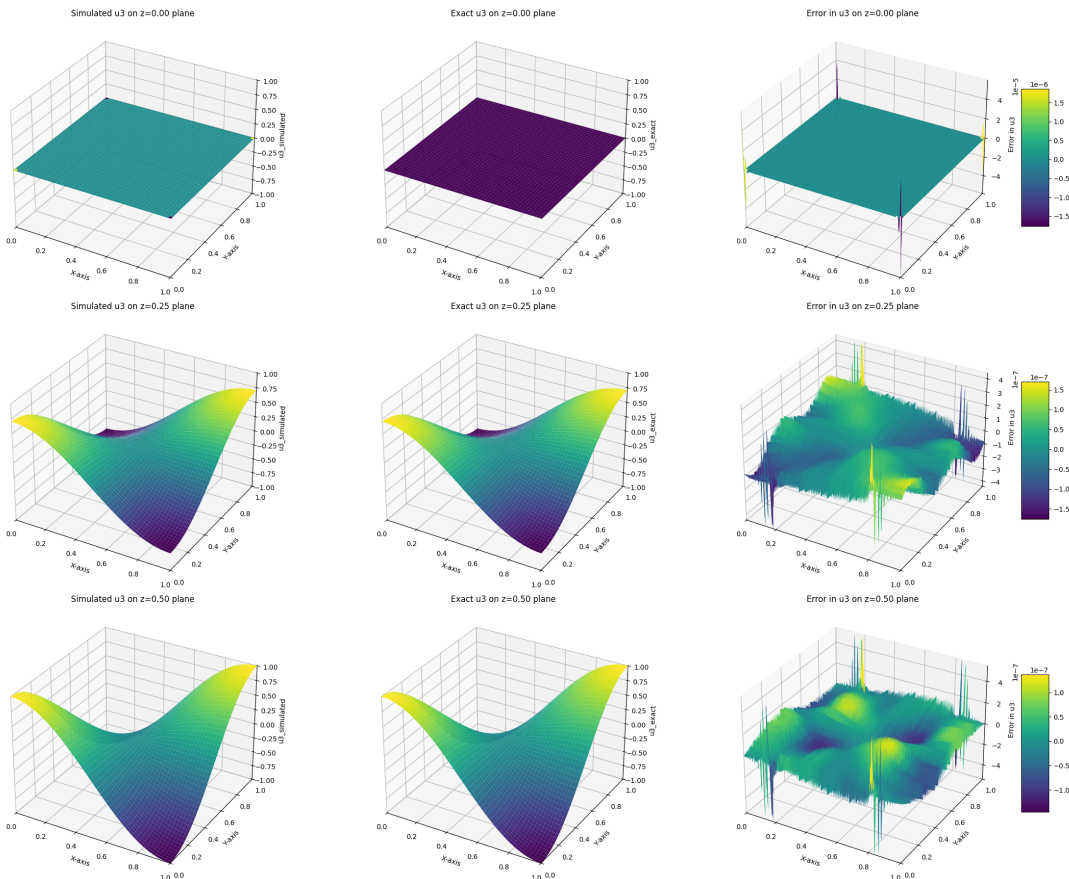


Figure 2.6: Plots comparison between the simulated and real $u_{e,3}$ with the error, for different plane z , with $d = 2$ and $n_{\text{cell}} = 128$

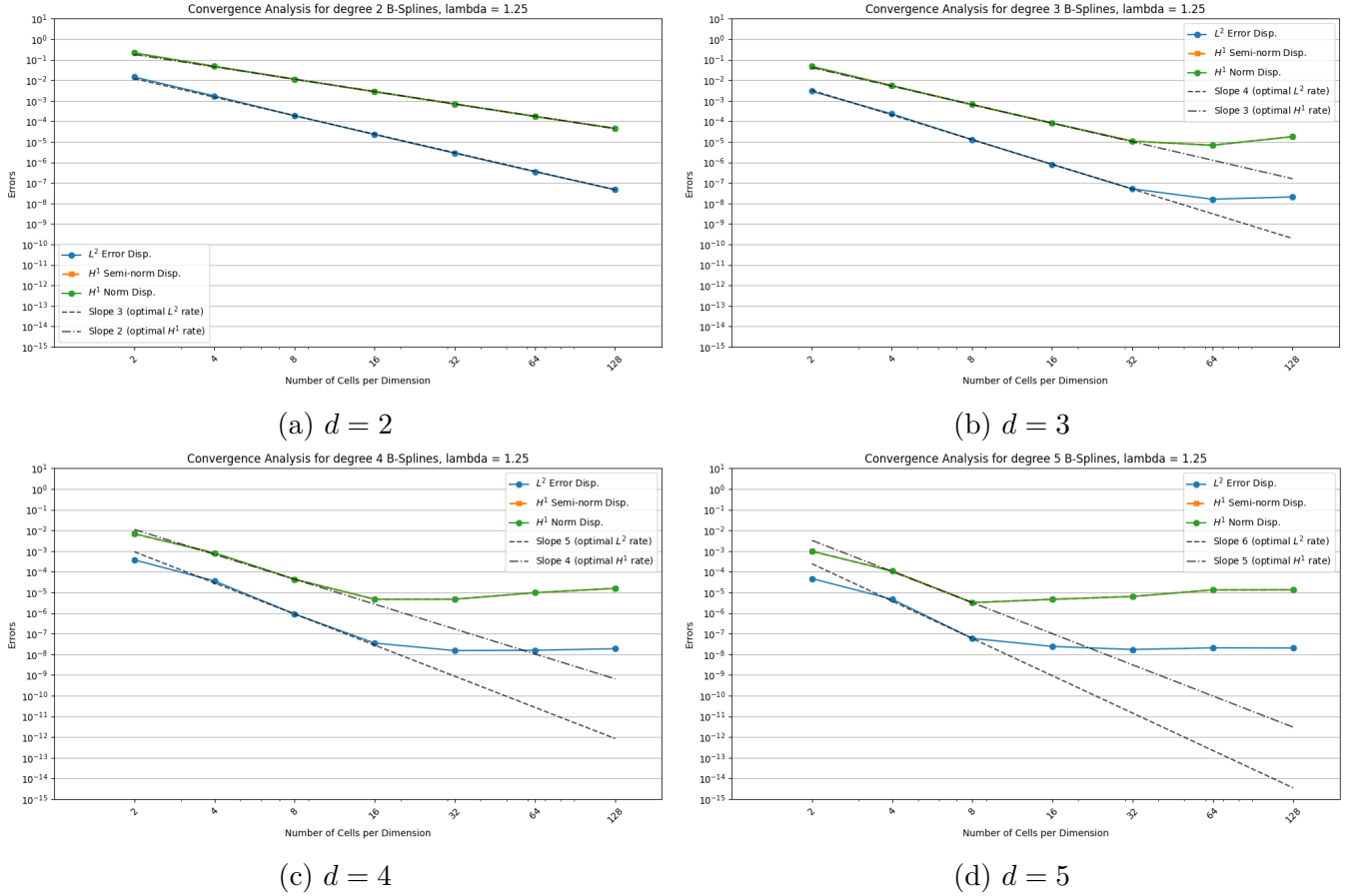


Figure 2.7: Four plots of relative errors ($\|\vec{u} - \vec{u}^h\|_{H^1(\Omega)}$ and $\|\vec{u} - \vec{u}^h\|_{L^2(\Omega)}$) with different degree B-Splines (with $\lambda = 1.25$ & $\mu = 1$)

For fixed value $\lambda = 1.25$ and $\mu = 1$, the codes seems to give a numerical solution that converges to the theoretical one with the expected order. We can notice that the plateau effect comes back and appears faster than in the case of Dirichlet Homogeneous Boundary Conditions. The L^2 error seems to converge to a value slightly higher than 10^{-8} , while the H^1 error converges to a value slightly higher than 10^{-5} , and this phenomena is more pronounced for higher degree B-Splines. The limit value of each error seems to be the same for all degree B-Splines, when the L^2 error becomes lower than 10^{-7} and the H^1 error becomes lower than 10^{-5} . So, this plateau effect is not due to the degree of B-Splines, but rather to the ill-conditionedness of the matrix of the bilinear form $a(.,.)$. This ill-conditionedness becomes worse with the refinement of the mesh and the increase of the degree of B-Splines. A way to verify this hypothesis is to solve the linear system with a different solver, with a preconditioner applyied to the matrix before the resolution.

These simulations have been made with $\lambda = 1.25$ and $\mu = 1$. We can now look at them for more realistic values of λ and μ . The following table 2.1 gives the Lamé coefficients for different materials.

Material	λ (GPa)	μ (GPa)
Steel	120	80
Concrete	17	14
Rubber	0.16	0.00033

Table 2.1: Lamé coefficients for different materials

But, the estimates (2.6) depends on $\frac{\lambda}{\mu}$, and when $\lambda \rightarrow +\infty$ (which is the case for incompressible

material), the estimates doesn't hold. Numerically, it is hard to get a value goes to $+\infty$, but for increasing values of λ , we can get plots from figure 2.8 below.

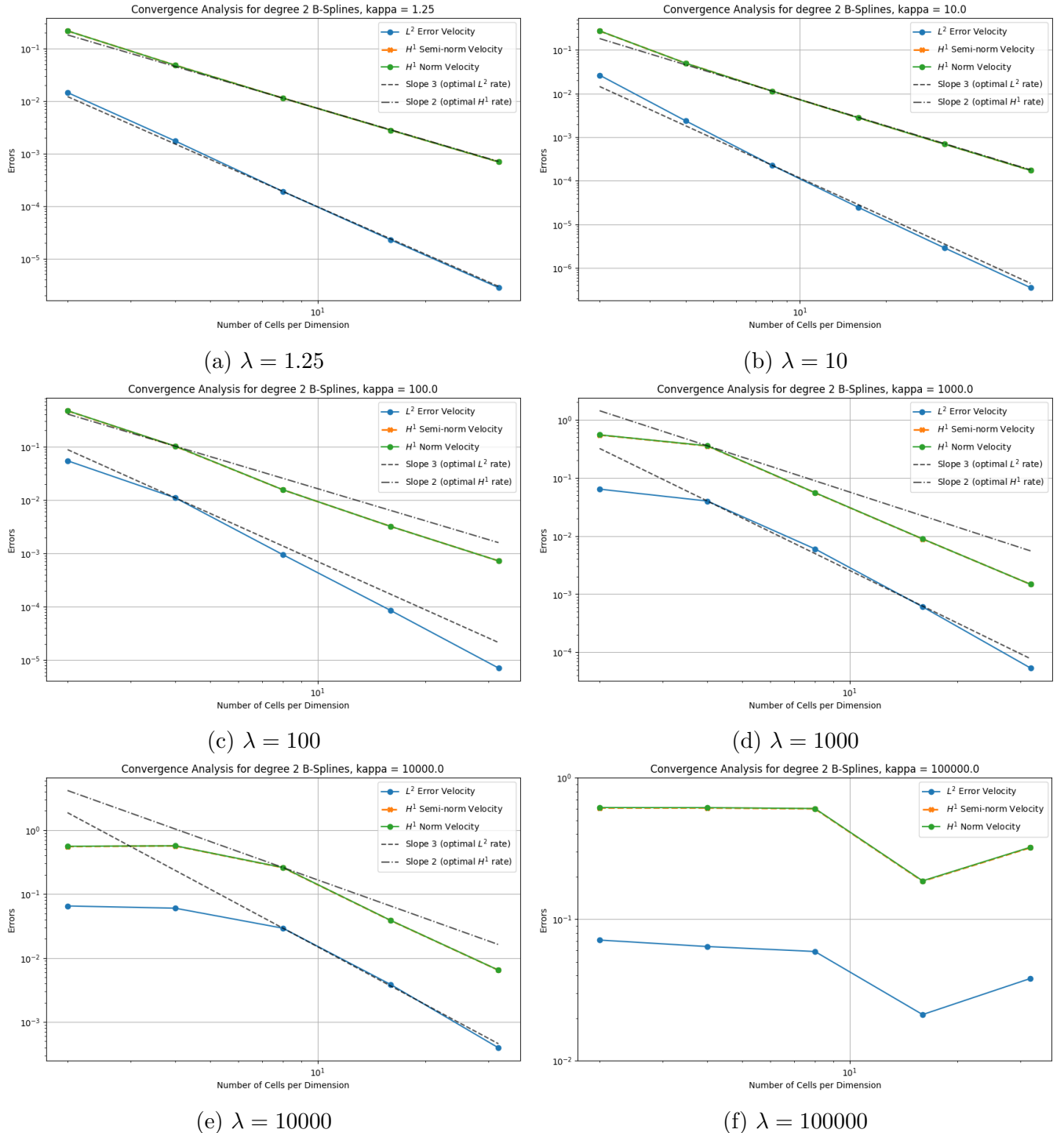


Figure 2.8: Error plots between exact solution and numerical solution with degree 2 B-Splines with increasing values of λ with $\mu = 1$

To compensate the problem of high values of λ , I have proposed to explore a Mixed Formulation by introducing a pressure field.

2.4 Mixed displacement-pressure formulation

To introduce this formulation, let's consider again the strong formulation from (2.3). Then, denotes by p the pressure field, defined by $p = -\lambda \nabla \cdot \vec{u}$. As we are seeking $\vec{u} \in \mathbf{H}^1(\Omega)$, p is naturally living in $L^2(\Omega)$. Then Hook's law can be rewritten : $\sigma(\vec{u}, p) = -pI_3 + 2\mu\varepsilon(\vec{u})$ in Ω
So the strong formulation can be re-write as : For a given $\vec{f} \in \mathbf{L}^2(\Omega)$, $\vec{t}_N \in \mathbf{L}^2(\partial\Omega_N)$, find $(\vec{u}, p) \in \mathbf{H}^1(\Omega) \times L^2(\Omega)$ such that :

$$\begin{cases} -\nabla \cdot \sigma(\vec{u}, p) = \vec{f} & \text{in } \Omega \quad (\text{Equilibrium}) \\ \nabla \cdot \vec{u} + \frac{1}{\lambda}p = 0 & \text{in } \Omega \quad (\text{Pressure field definition}) \\ \vec{u} = \vec{0} & \text{in } \partial\Omega_D \\ \sigma(\vec{u}) \cdot \vec{n} = \vec{t}_N & \text{in } \partial\Omega_N \end{cases} \quad (2.7)$$

Now, to derive the weak formulation associated, first we multiply the Equilibrium equation by $v \in \mathbf{H}_{0,D}^1(\Omega)$ and we interger by part on Ω , then we multiply the Pressure field equation by $q \in L^2(\Omega)$ and we interger over Ω . Then we just have to add both integrals. Then, the weak formulation is:

$$\begin{cases} \text{Find } (\vec{u}, p) \in \mathbf{H}_{0,D}^1(\Omega) \times L^2(\Omega) \text{ such that :} \\ \tilde{a}((\vec{u}, p), (\vec{v}, q)) = l(\vec{v}, q) \quad \forall (\vec{v}, q) \in \mathbf{H}_{0,D}^1(\Omega) \times L^2(\Omega) \end{cases} \quad (2.8)$$

With :

$$\begin{aligned} \tilde{a} : & \left\{ \begin{array}{l} (\mathbf{H}_{0,D}^1(\Omega) \times L^2(\Omega))^2 \rightarrow \mathbb{R} \\ ((\vec{u}, p), (\vec{v}, q)) \mapsto \int_{\Omega} \left(2\mu\varepsilon(\vec{u}) : \varepsilon(\vec{v}) - p(\nabla \cdot \vec{v}) + (\nabla \cdot \vec{u})q + \frac{1}{\lambda}pq \right) dV \end{array} \right. \\ l : & \left\{ \begin{array}{l} \mathbf{H}_{0,D}^1(\Omega) \rightarrow \mathbb{R} \\ \vec{v} \mapsto \int_{\Omega} \vec{f} \cdot \vec{v} dV + \int_{\partial\Omega_N} \vec{t}_N \cdot \vec{v} dS \end{array} \right. \end{aligned}$$

The well-posedness of this new mixed-problem can be proven by the way as the pure displacement problem in **Section 2.2**.

2.4.1 Example of simulation using PSYDAC

I have first try to implement the previous formulation with same hypothesis as in **Subsection 2.3.1**. In this case, the known pressure field is defined as :

$$p_e = -\lambda\pi \sin(\pi x) \sin(\pi y) \cos(\pi z)$$

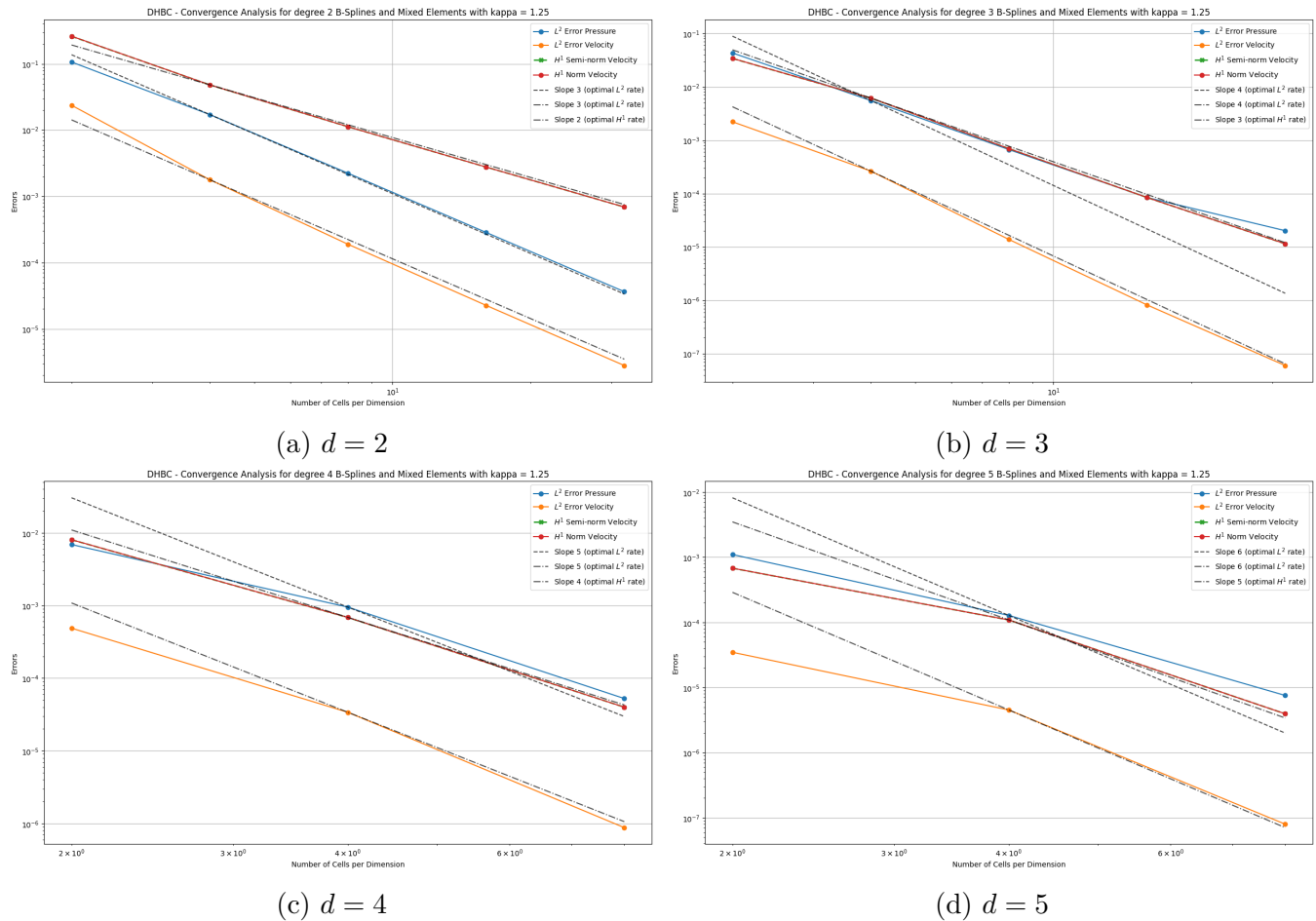


Figure 2.9: Four plots of errors between exact solution and numerical solution with different degree B-Splines (with $\lambda = 1.25$ & $\mu = 1$) using the mixed formulation

Compare these two formulation in "extreme" cases on the supercomputer ?

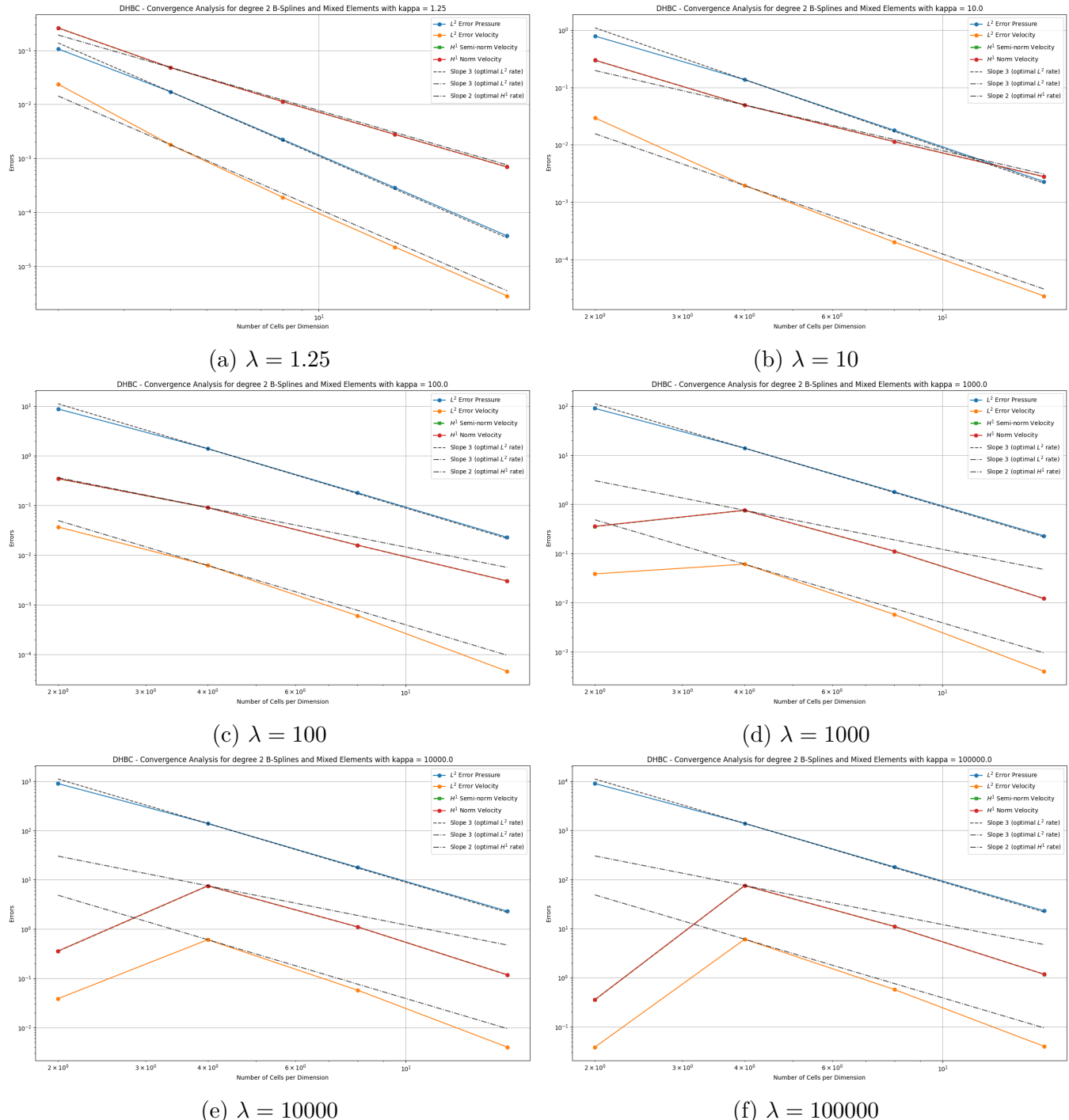


Figure 2.10: Error plots between exact solution and numerical solution with degree 2 B-Splines and mixed formulation with increasing values of λ

Chapter 3

References

- [EG04] Alexandre Ern and Jean-Luc Guermond. *Theory and Practice of Finite Elements*. en. Ed. by S. S. Antman, J. E. Marsden, and L. Sirovich. Vol. 159. Applied Mathematical Sciences. New York, NY: Springer New York, 2004. ISBN: 978-1-4419-1918-2 978-1-4757-4355-5. DOI: 10.1007/978-1-4757-4355-5. URL: <http://link.springer.com/10.1007/978-1-4757-4355-5> (visited on 06/16/2025).
- [BS08] Susanne C. Brenner and L. Ridgway Scott. *The Mathematical Theory of Finite Element Methods*. en. Ed. by J. E. Marsden, L. Sirovich, and S. S. Antman. Vol. 15. Texts in Applied Mathematics. New York, NY: Springer New York, 2008. ISBN: 978-0-387-75933-3 978-0-387-75934-0. DOI: 10.1007/978-0-387-75934-0. URL: <http://link.springer.com/10.1007/978-0-387-75934-0>.
- [Gou13] Phillip L. Gould. *Introduction to Linear Elasticity*. en. New York, NY: Springer New York, 2013. ISBN: 978-1-4614-4832-7 978-1-4614-4833-4. DOI: 10.1007/978-1-4614-4833-4. URL: <https://link.springer.com/10.1007/978-1-4614-4833-4>.
- [Da +14] L. Beirão Da Veiga et al. “Mathematical analysis of variational isogeometric methods”. en. In: *Acta Numerica* 23 (May 2014), pp. 157–287. ISSN: 0962-4929, 1474-0508. DOI: 10.1017/S096249291400004X. URL: https://www.cambridge.org/core/product/identifier/S096249291400004X/type/journal_article (visited on 06/26/2025).
- [Cin18] Emma Cinatl. “Finite Element Discretizations for Linear Elasticity”. en. PhD thesis. Clemson University, 2018.
- [GHR22] Y. Güclü, S. Hadjout, and A. Ratnani. “PSYDAC: a high-performance IGA library in Python”. en. In: *8th European Congress on Computational Methods in Applied Sciences and Engineering*. CIMNE, 2022. DOI: 10.23967/eccomas.2022.227. URL: https://www.scipedia.com/public/Guclu_et_al_2022a (visited on 06/17/2025).
- [Che24] Long Chen. “Variational Formulation of linear elasticity”. en. In: (2024).

Chapter 4

Appendices

4.1 Other plots of solutions for the problem with Dirichlet Homogeneous Boundary Conditions